

1 **Ice core evidence for decoupling between mid-latitude atmospheric water cycle and Greenland**
2 **temperature during the last deglaciation**

3 Amaëlle Landais^{1,*}, Emilie Capron^{2,3}, Valérie Masson-Delmotte¹, Samuel Toucanne⁴, Rachael
4 Rhodes⁵, Trevor Popp², Bo Vinther², Bénédicte Minster¹, Frédéric Prié¹

5 ¹ Laboratoire des Sciences du Climat et de l'Environnement, IPSL, UMR 8212, CEA-CNRS-UVSQ-UPS,
6 Gif sur Yvette, France

7 ² Centre for Ice and Climate, Niels Bohr Institute, University of Copenhagen, Juliane Maries Vej 30,
8 DK-2900, Copenhagen, Denmark;

9 ³ British Antarctic Survey, High Cross, Madingley Road, Cambridge, CB3 0ET, UK

10 ⁴ IFREMER, Laboratoire Géophysique et enregistrement Sédimentaire, CS 10070, 29280 Plouzané,
11 France

12 ⁵ Department of Earth Sciences, University of Cambridge, Downing Street, Cambridge, CB2 3EQ
13 UK

14

15 * Corresponding author: phone : +33 (0)169084672, email : amaelle.landais@lsce.ipsl.fr, ORCID :
16 0000-0002-5620-5465

17 Keywords: Deglaciation, Water isotopes, ¹⁷O-excess, d-excess, Heinrich event, Mystery interval

18

19 **Abstract**

20 The last deglaciation represents the most recent example of natural global warming associated with
21 large-scale climate changes. In addition to the long-term global temperature increase, the last
22 deglaciation onset is punctuated by a sequence of abrupt changes in the Northern Hemisphere. Such
23 interplay between orbital- and millennial-scale variability is widely documented in paleoclimatic
24 records but the underlying mechanisms are not fully understood. Limitations arise from the difficulty
25 in constraining the sequence of events between external forcing, high- and low- latitude climate and
26 environmental changes.

27 Greenland ice cores provide sub-decadal-scale records across the last deglaciation and contain
28 fingerprints of climate variations occurring in different regions of the Northern Hemisphere. Here, we
29 combine new ice δ -excess and ^{17}O -excess records, tracing changes in the mid-latitudes, with ice $\delta^{18}\text{O}$
30 records of polar climate. Within Heinrich Stadial 1, we demonstrate a decoupling between climatic
31 conditions in Greenland and those of the lower latitudes. While Greenland temperature remains
32 mostly stable from 17.5 to 14.7 ka, significant change in the mid latitudes of northern Atlantic takes
33 place at ~ 16.2 ka, associated with warmer and wetter conditions of Greenland moisture sources. We
34 show that this climate modification is coincident with abrupt changes in atmospheric CO_2 and CH_4
35 concentrations recorded in an Antarctic ice core. Our coherent ice core chronological framework and
36 comparison with other paleoclimate records suggests a mechanism involving two-step freshwater
37 fluxes in the North Atlantic associated with a southward shift of the intertropical convergence zone.

38

39 **Introduction**

40 The last deglaciation (~19 thousand to 11 thousand years before present, ka) is the most recent major
41 reorganization of global climate and is thus extensively documented by proxy records from natural
42 climate archives. The wealth of high-resolution records from well-dated archives and data synthesis
43 obtained over the past decades show two modes of climate variability during this period (e.g. Denton
44 et al., 2010, Clark et al., 2012). The first is a long-term increase in global surface temperature and
45 atmospheric CO₂ concentration between 18 and 11 ka. Superimposed on this is a sequence of
46 centennial-scale transitions between three quasi-stable intervals documented in Northern
47 Hemisphere temperature, namely (i) the Heinrich Stadial 1 (~17.5-14.7 ka), that encompasses the
48 massive rafting episode known as Heinrich event 1 (from ~16 ka); (ii) the Bølling-Allerød warming phase
49 (~14.7 to 12.9 ka) and (iii) the Younger Dryas cold phase (~12.9 to 11.7 ka). This three-step sequence
50 coincides with rapid variations in the Atlantic Meridional Oceanic Circulation (AMOC) (Mc Manus et
51 al., 2004), with evidence for a weak meridional overturning in the North Atlantic during the cold period
52 encompassing Heinrich Stadial 1 and the Younger Dryas.

53 Our understanding of the mechanisms at play during these North Atlantic cold phases remains limited.
54 First, recent studies challenge the earlier attribution of the AMOC slowdown during Heinrich Stadial 1
55 to the impact of the Iceberg Rafted Debris (IRD) from the Laurentide ice sheet through Hudson Strait
56 (Alvarez-Solas et al., 2011). In particular, meltwater releases from the European ice sheet occurring as
57 early as 19 or 20 ka may have played an important role in this AMOC slowdown (Toucanne et al., 2010;
58 Stanford et al., 2011; Hodell et al., 2017).

59 Second, major global reorganizations of the hydrological cycle have been demonstrated during
60 Heinrich Stadial 1. They can be separated in two phases. In North America, a first time interval
61 characterized by low lake levels (referred to as the “big dry”, 17.5 to 16.1 ka) was followed by a second
62 time interval with high lake levels (referred to as the “big wet”, 16.1 to 14.7 ka) (Broecker et al., 2012),

63 both apparently occurring during a stable cold phase in Greenland temperature. The second phase of
64 Heinrich Stadial 1 is also associated with a weak East Asian monsoon interval (Zhang et al., 2014),
65 understood to reflect a southward shift of the Inter-tropical Convergence Zone (ITCZ). While there is
66 growing evidence for large-scale reorganizations of climate and low- to mid- latitude atmospheric
67 water cycle within Heinrich Stadial 1, the exact sequence of events is not known with sufficient
68 accuracy to understand the links between changes in North Atlantic climate, AMOC, and the lower
69 latitude water cycle.

70 Linking changes in the high latitudes of the North Atlantic and the mid- to low- latitudes requires
71 precise absolute chronologies such as those obtained from annual layer counting of Greenland ice (e.g.
72 Andersen et al., 2006) or U/Th dating of speleothems (e.g. Zhang et al., 2014). Unfortunately, absolute
73 dating uncertainties increase above a hundred years during the last deglaciation, precluding a direct
74 comparison of proxy records at the centennial scale. In this study, we circumvent this difficulty by using
75 proxy records measured on Greenland ice cores that represent both Greenland temperature and mid-
76 latitude moisture source conditions.

77 **Analytical method**

78 Here, we present new water isotope records ($\delta^{18}\text{O}$, d-excess = $\delta\text{D} - 8 \times \delta^{18}\text{O}$, ^{17}O -excess = $\ln(\delta^{17}\text{O} + 1) -$
79 $0.528 \times \ln(\delta^{18}\text{O} + 1)$) from the NGRIP ice core (NGRIP et al., 2004), reported on the annual-layer counted
80 Greenland Ice Core Chronology 2005 (hereafter GICC05, Rasmussen et al., 2006; Svensson et al., 2008),
81 and associated with relatively small absolute uncertainties over the last deglaciation (maximum
82 counting error of 100-200 yr). Other Greenland and Antarctic ice cores have been aligned on the
83 GICC05 chronology, with a maximum relative dating uncertainty of 400 years over the last deglaciation
84 (Rasmussen et al., 2008; Bazin et al. 2013; Veres et al., 2013).

85 The new NGRIP $\delta^{18}\text{O}$ and δD dataset was obtained at Laboratoire des Sciences du Climat et de
86 l'Environnement (LSCE) using a PICARRO laser cavity ring-down spectroscopy (CRDS) analyzer. The
87 accuracy for $\delta^{18}\text{O}$ and δD measurements displayed here is about 0.1‰ and 1‰ respectively. This new

88 dataset completes the NGRIP high-resolution isotopic dataset published over the time period 11.5 to
89 14.7 ka with $\delta^{18}\text{O}$ and δD measured respectively at the University of Copenhagen and at the Institute
90 of Arctic and Alpine Research (INSTAAR) Stable Isotope Lab (SIL) (University of Colorado). $\delta^{18}\text{O}$ analyses
91 were performed at the Niels Bohr Institute (University of Copenhagen) using a CO_2 equilibration
92 technique (Epstein et al., 1953) with an analytical precision of 0.07‰. δD measurements at INSTAAR
93 were made via an automated uranium reduction system coupled to a VG SIRA II dual inlet mass
94 spectrometer (Vaughn et al., 1998). Analytical precision for δD is $\pm 0.5\%$ or better. Both timeseries
95 show similar $\delta^{18}\text{O}$ values, in agreement with the reference $\delta^{18}\text{O}$ series for NGRIP over the last climatic
96 cycle (NGRIP community members, 2004) within error bars. However, while both LSCE and INSTAAR
97 SIL d-excess timeseries display the same 3.5‰ decrease over the onset of Bølling-Allerød, the mean d-
98 excess level differs by 2.5‰ between the two records. Despite several home standard intercalibrations
99 between the two laboratories, this difference remains unexplained and prevents any further discussion
100 on the absolute NGRIP d-excess levels. The new and published NGRIP d-excess dataset are combined
101 after a shift of the INSTAAR SIL d-excess series by -2.5‰.

102 In order to perform ^{17}O -excess measurements on water samples at LSCE, we follow the method
103 described in details in (Barkan and Luz, 2005). In short, for each sample, 2 μL of water are injected in
104 a helium flow purified by passing through a trap immersed in liquid nitrogen. Water vapor then reacts
105 with CoF_3 (producer Sigma-Aldrich) in a nickel tube heated at 370°C to produce oxygen and fluorhydric
106 acid which is trapped in liquid nitrogen at the outlet of the nickel tube. Oxygen is first trapped in a
107 molecular sieve tube immersed in liquid nitrogen and then separated from helium and purified through
108 two cycles of warming (+30°C) and cooling (-196°C) of the tube with molecular sieves. The oxygen is
109 finally trapped in a manifold immersed in liquid helium. After warming the manifold at least 40 minutes
110 at room temperature, the triple isotopic composition of produced oxygen is injected in the mass
111 spectrometer (MAT 253) and measured by dual inlet against a reference O_2 gas (two runs of 20
112 measurements).

113 Every day, at least one home standard is run with the batch of samples to check the stability of the
114 fluorination line and mass spectrometer. In addition, a series of three water home standards, whose
115 $\delta^{18}\text{O}$ and $\delta^{17}\text{O}$ values are calibrated on the SMOW – SLAP scale following Schoenemann et al. (2013),
116 is run at least every month. For this study, the SMOW – SLAP calibrated home standards have $\delta^{18}\text{O}$
117 values of respectively -18.64 ‰, -33.56 ‰ and -54.05 ‰, hence bracketing the $\delta^{18}\text{O}$ values of the
118 measured samples. The comparison of the measured and SMOW-SLAP calibrated $\delta^{18}\text{O}$ and $\delta^{17}\text{O}$ values
119 then enables calibrating the $\delta^{18}\text{O}$ and ^{17}O -excess values of the NGRIP samples following the method
120 described in (Schoenemann et al., 2013; Landais et al., 2014). The resulting mean uncertainty is of 5
121 ppm (1σ) for the ^{17}O -excess measurements of this study. Note that the use of the MAT 253 mass
122 spectrometer gave more stable results than a Delta V+ instrument used for previous studies at LSCE
123 (e.g. Landais et al., 2012).

124 **Results: water isotopic records at NGRIP**

125 Our 1518 new measurements of $\delta^{18}\text{O}$ and d-excess on the NGRIP ice core cover the time period 14.5
126 to 60 ka (Figure 1) and we present 435 duplicate measurements of ^{17}O -excess over the time period
127 ranging from 9.6 to 20 ka (Figure 2). $\delta^{18}\text{O}$ is a qualitative proxy for local surface temperature.
128 Comparisons between ice core $\delta^{18}\text{O}$ data and paleotemperature estimates from borehole temperature
129 profile inversion and abrupt temperature changes inferred from isotopic measurements on trapped
130 air showed that the $\delta^{18}\text{O}$ -temperature relationship at NGRIP varies from 0.3 to 0.5 ‰.°C⁻¹ during
131 glacial-interglacial periods (Buizert et al., 2014; Dahl-Jensen et al., 1998; Kindler et al., 2014).

132 The second-order parameter d-excess (Dansgaard, 1964) is used in Greenland ice cores to track past
133 changes in evaporation conditions or shifts in moisture sources (Johnsen et al., 1989; Masson-
134 Delmotte et al., 2005a). Evaporation conditions affect the initial vapor d-excess through the impact of
135 surface humidity and sea surface temperature on kinetic fractionation (Jouzel et al., 1982). Recent
136 vapour monitoring and modelling studies show that the d-excess signal of the moisture source can be
137 preserved in polar vapour and precipitation after transportation towards polar regions (Bonne et al.,

138 2015; Pfahl and Sodemann, 2014). This signal can however be altered during distillation due to the
139 sensitivity of equilibrium fractionation coefficients to temperature, leading to alternative definitions
140 using logarithm formulations for Antarctic ice cores (Uemura et al., 2012; Markle et al., 2016). Finally,
141 changes in $\delta^{18}\text{O}_{\text{sea water}}$ also influence $\delta^{18}\text{O}$ and d-excess in polar precipitation. Summarizing, d-excess in
142 Greenland ice core is a complex tracer: interpreting its past variations in terms of changes in
143 evaporation conditions (sea surface temperature or humidity) requires deconvolution of the effects of
144 glacial-interglacial changes in $\delta^{18}\text{O}_{\text{sea water}}$ and condensation temperature.

145 ^{17}O -excess provides complementary information to d-excess (Landais et al., 2008; Landais et al., 2012).
146 At evaporation, d-excess and ^{17}O -excess are both primarily influenced by the balance between kinetic
147 and equilibrium fractionation, itself driven by relative humidity at the sea surface. During transport,
148 while d-excess is influenced by distillation effects during atmospheric cooling, ^{17}O -excess is largely
149 insensitive to this effect, except at very low temperatures in Antarctica (Winkler et al., 2012).
150 Conversely, ^{17}O -excess is affected by recycling or mixing of air masses along the transport path from
151 low to high latitudes (Risi et al., 2010), and by the range over which supersaturated conditions occur,
152 itself affected for instance by changes in sea-ice extent or temperature along the transport path
153 (Schoenemann et al., 2014). Because of its logarithmic definition, ^{17}O -excess is not sensitive to changes
154 in $\delta^{18}\text{O}_{\text{sea water}}$ given that the ^{17}O -excess of global sea water remains constant with time. As a
155 consequence, a change in sea water isotopic composition will only be transmitted to the ^{17}O -excess of
156 the precipitation if the ^{17}O -excess of the evaporated sea-water is modified.

157 As previously reported for the central Greenland GRIP ice core (Masson-Delmotte et al., 2005b; Jouzel
158 et al., 2005), the NGRIP $\delta^{18}\text{O}$ and d-excess records exhibit a systematic anti-correlation during the
159 abrupt Dansgaard-Oeschger (DO) events of the last glacial period and last deglaciation (Bølling-Allerød
160 and Younger Dryas), with d-excess being higher during cool Greenland Stadials and lower during warm
161 Greenland Interstadials.

162 The origin of moisture may be different at GRIP and NGRIP. While both sites are expected to receive
163 most of their moisture from the North Atlantic and North America (Werner et al., 2001, Landais et al.,
164 2012, Langen and Vinther, 2009) with modulation partly linked to sea ice extent (Rhines et al., 2014),
165 the northwestern NGRIP site may also receive moisture from North Pacific (Langen and Vinther, 2009).
166 Nevertheless, the two sites depict similar amplitudes of d-excess variations across DO events (Figure
167 1). We note that this contrasts with a slightly lower amplitude (typically by 1‰) of abrupt $\delta^{18}\text{O}$ changes
168 at NGRIP compared to GRIP.

169 The fact that d-excess increases (by 3.5 ± 1 ‰) when $\delta^{18}\text{O}$ decreases (by 4 ± 1 ‰) during Greenland
170 Stadials relative to interstadials may at least partly reflect the influence of local temperature changes
171 on d-excess, challenging a simple interpretation in terms of changes in source conditions. We note one
172 exception, the Heinrich Stadial 1 cold phase preceding the onset of the Bølling-Allerød at 14.7 ka.
173 During the time interval 17.5 to 14.7 ka, the $\delta^{18}\text{O}$ values measured in the three Greenland ice cores
174 NGRIP, GRIP and GISP2 remains almost stable (Figure 2). Over this period, $\delta^{18}\text{O}$ variations are smaller
175 than 1 ‰, i.e. less than one fourth of the average amplitude in $\delta^{18}\text{O}$ changes across DO events,
176 suggesting no large temperature change in Greenland during this period. The link between flat $\delta^{18}\text{O}$
177 and minimal temperature variability can be challenged since a mean temperature signal can be masked
178 by a change in seasonality of moisture source origin on the $\delta^{18}\text{O}$ record (Boyle et al., 1994; Krinner et
179 al., 1997). However, our assumption of stable temperature is supported by constant $\delta^{15}\text{N}$ of N_2 values
180 in the GISP2 and NGRIP ice cores (Buizert et al., 2014), $\delta^{15}\text{N}$ of N_2 being an alternative
181 paleothermometry tool in ice core that is not affected by processes within the water cycle
182 (Severinghaus and Brook, 1999). In contrast to this almost stable $\delta^{18}\text{O}$ signal, d-excess depicts an
183 average 2.2 ‰ increase at 16.1 ka (more than 60% of the average amplitude during DO events) with a
184 larger amplitude at GRIP (2.7 ‰) than at NGRIP (1.7 ‰) (Figure 2). In this case, the increase in d-excess
185 cannot be explained by any Greenland temperature change, and therefore demonstrates a decoupling
186 between cold and stable Greenland temperatures and changing climatic conditions at lower latitudes
187 during Heinrich Stadial 1 (see also SOM).

188 While the ^{17}O -excess level is similar at the Last Glacial Maximum (i.e. before 19 ka on Figure 2) and the
189 Early Holocene (40 ppm), it also shows significant variations during the last deglaciation. Most of these
190 variations co-vary with those of $\delta^{18}\text{O}$ such as the four main oscillations during the Bølling-Allerød and
191 the onset and end of the Younger Dryas. They can be interpreted as parallel variations in the Greenland
192 temperature and lower latitude climate with a possible contribution of local temperature through
193 kinetic effects. Again, a major difference occurs during Heinrich Stadial 1. While the $\delta^{18}\text{O}$ record is
194 relatively stable, the ^{17}O -excess profile exhibits a decreasing trend (strongest between 17.5 and 16.1
195 ka) before a minimum level is reached between 16.1 to 14.7 ka. We therefore observe a clear and
196 synchronous signal in both d-excess and ^{17}O -excess dated around 16.2 ka from statistical analysis (cf.
197 section 1 in SOM).

198 **Discussion**

199 The ^{17}O -excess and d-excess transitions at 16.2 ka do not have any clear counterpart in $\delta^{18}\text{O}$ (cf section
200 2 in SOM) and no temperature variation at that time was recorded in the $\delta^{15}\text{N}$ of N_2 record. We
201 interpret these patterns as illustrating a reorganization of climatic conditions and/or water cycle at
202 latitudes south of Greenland. A similar shift in ^{17}O -excess has already been observed during Heinrich
203 Stadial 4 in the NEEM ice core, while the $\delta^{18}\text{O}$ record exhibits a constant low level (Guillevic et al.,
204 2014). This pattern was also attributed to a change in the water cycle and/or climate at lower latitudes.

205 The Greenland water stable isotope records demonstrate a change in the water cycle and/or climate
206 at lower latitudes at 16.2 ka when Greenland conditions were relatively stable and cold. This change
207 at low latitudes is confirmed by the high resolution atmospheric CH_4 concentration record from the
208 WAIS Divide ice core (Rhodes et al., 2015) (Figure 2). At 16.2 ka, the CH_4 record indeed exhibits a 30
209 ppbv peak hypothesized to reflect more CH_4 production in Southern Hemisphere wetlands, driven by
210 wetter conditions due to a southward shift of the tropical rainbelts associated with the ITCZ (Rhodes
211 et al., 2015). The parallel increase of atmospheric CO_2 concentration by 10 ppm in ~ 100 years (Marcott
212 et al., 2013) is understood to result from increased terrestrial carbon fluxes or enhanced air-sea gas

213 exchange in the Southern Ocean (Bauska et al., 2014). We also highlight an unusual characteristic of
214 the bipolar seesaw pattern in Antarctic ice core $\delta^{18}\text{O}$ records at 16.2 ka. As observed during all
215 Greenland Stadials of the last glacial period, Antarctic $\delta^{18}\text{O}$ also increases during Heinrich Stadial 1 (e.g.
216 EPICA community members, 2006), through the warming phase of Antarctic Isotopic Maximum 1. The
217 EPICA Dronning Maud Land (EDML) ice core, drilled in the Atlantic sector of Antarctica, shows an
218 associated two step $\delta^{18}\text{O}$ increase. The first step, marked by a strong increasing trend, is followed by a
219 change in slope at 16.2 ka. The second step is characterized by a slower increasing trend from 16.2 to
220 14.7 ka (EPICA community members, 2006; Stenni et al., 2011) (Figure 2). The EDML $\delta^{18}\text{O}$ variations
221 are expected to be closely connected to changes in AMOC due to the position of the ice core site on
222 the Atlantic sector of the East Antarctic plateau and a link between EDML $\delta^{18}\text{O}$ record and low latitude
223 signal over Heinrich Stadial 1 has already been suggested by Zhang et al. (2016). For other Antarctic
224 sites, the change of slope around 16.2 ka is less clear, probably due to the damping effect of the
225 Southern Ocean or because other climatic effects linked to atmospheric teleconnections with the
226 tropics affect the Pacific and Indian sectors of Antarctica (Stenni et al., 2011, WAIS Divide members,
227 2013; Buiron et al., 2012). A change in the teleconnections between West Antarctic climate and
228 tropical regions is also observed around 16.2 ka (Jones et al., 2018). Summarizing, our synthesis of ice
229 core records clearly demonstrates a climate shift at 16.2 ka, identified in proxy records sensitive to
230 shifts in tropical hydrology (CH_4), mid-latitude hydrological cycle changes in the Atlantic basin
231 (Greenland second order isotopic tracers), as well as in Antarctic climate dynamics in the Atlantic basin.
232 This suggests some reorganization of water cycle in the Atlantic region (possibly involving AMOC)
233 related to surface shifts in the ITCZ at 16.2 ka. This does not appear to affect the high latitudes of the
234 North Atlantic as Greenland temperatures stay uniformly cold. Uniformly cold conditions in Greenland
235 are generally observed during Heinrich Stadials of the last glacial period with temperature and $\delta^{18}\text{O}$
236 levels that are not significantly lower than temperature levels observed during Greenland Stadials
237 (Kindler et al., 2014; Guillevic et al., 2014). Because Greenland is surrounded by large sea ice during
238 Greenland Stadials and Heinrich Stadials (Hoff et al., 2016), an explanation may be that central

239 Greenland temperatures are saturated during cold periods so that AMOC modifications occurring
240 south of the sea ice edge are not influencing significantly Greenland temperatures. During Heinrich 1
241 occurring during the last deglaciation, the situation may be more complicated because of the CO₂
242 concentration and insolation increases. In this case, the occurrence of Heinrich Stadial 1 may
243 counteract the increase in Greenland temperature records induced by CO₂ and insolation forcing
244 through winter cooling driven by AMOC weakening as suggested by Buizert et al. (2018).

245 At low latitudes, an ITCZ shift at 16.2 ka is clearly expressed through a weak monsoon interval in East
246 Asian speleothem records and through change in hydrology in the low-latitude Pacific region, Cariaco
247 Basin and Brazil (Partin et al., 2007; Deplazes et al., 2013; Russell et al., 2014; Strikis et al., 2015). Since
248 we have ruled out a local temperature signal at 16.2 ka in Greenland, the origin of the Greenland d-
249 excess and ¹⁷O-excess changes around 16.2 ka is also linked to changes in the climate of the source
250 evaporative regions. When evaporation conditions change, they affect the proportion of kinetic versus
251 equilibrium fractionation, and cause similar trends in both d-excess and ¹⁷O-excess. Both of them
252 indeed increase when kinetic fractionation is more important, i.e. when relative humidity decreases,
253 or when a change in sea ice modifies the evaporative conditions (Klein et al., 2015; Kopec et al., 2016).
254 However, d-excess in the atmospheric vapor is affected by distillation toward higher latitudes, and
255 strongly depends on the source-site temperature gradient, while ¹⁷O-excess preserves better the initial
256 fingerprint of relative humidity of the evaporative region.

257 As a result, the opposing trends observed in d-excess and ¹⁷O-excess at 16.2 ka can most probably be
258 explained by an increase of both the relative humidity and the sea surface temperature of the
259 evaporative source regions for Central and North Greenland. Despite known limitations (Winkler et al.,
260 2012, Schoenemann and Steig, 2016), the classical approach for inferring changes in source relative
261 humidity and surface temperature from d-excess and ¹⁷O-excess in Greenland (Masson-Delmotte et
262 al., 2005a; Landais et al., 2012) suggests respective increases of the order of 3°C and 8% for
263 temperature and relative humidity of the source evaporative regions respectively. The larger d-excess

264 increase at the transition between Phase 1 and Phase 2 of Heinrich Stadial 1 observed at GRIP
265 compared to NGRIP is compatible with a larger proportion of GRIP moisture provided by the mid-
266 latitude North Atlantic for this site. A larger increase in the sea surface temperature of the source of
267 moisture for GRIP compared to NGRIP would also reduce the source-site temperature gradient and is
268 fully compatible with the 2 ‰ less depleted level of $\delta^{18}\text{O}$ at GRIP, compared to NGRIP, during Phase 2.
269 The increases in both temperature and relative humidity of the Greenland source regions suggest a
270 more intense evaporative flux from lower latitudes starting at 16.2 ka. Such features could be
271 explained either by a local climate signal of evaporative regions or by a southward shift of evaporative
272 source regions toward warmer and more humid locations. The signal of source temperature increase
273 is in line with earlier interpretations of Greenland d-excess changes (Steffensen et al., 2018; Masson-
274 Delmotte et al., 2005b). The signal of source humidity increase may at least partly explained by wetter
275 conditions in the continental North America evaporative source regions, which are known to partly
276 affect Greenland moisture today in addition to the main source in Northern Atlantic (Werner et al.,
277 2001; Langen and Vinther, 2009). This relative humidity signal reconstructed from Greenland ^{17}O -
278 excess at the transition between Phase 1 and Phase 2 of Heinrich Stadial 1 coincides with the onset of
279 the “big wet” period in North American records (Broecker and Putnam, 2012). This transition to a big
280 wet period can be explained by a southward shift of the storm tracks and polar jet stream over North
281 America shift during this period (Asmerom et al., 2010).

282 We now explore paleoceanographic records to search for a fingerprint of climate and/or AMOC
283 reorganization at 16.2 ka in the North Atlantic region and possible implications for our ice core records.
284 Such comparison of ice core and marine sediment records appears insightful despite existing
285 limitations attached to relative chronologies. First, high resolution proxy records of surface sea
286 temperature in the East Atlantic, near Europe, depict a clear warming in the middle of Heinrich Stadial
287 1 (Bard et al., 2000; Matrat et al., 2014, Figure 3). This signal is coherent with our interpretation of
288 Greenland d-excess increase at 16.2 ka. In the deep Western Atlantic, no specific feature emerges

289 between Phase 1 and Phase 2 of Heinrich Stadial 1 from the multi-centennial resolution record of
290 Pa/Th, a proxy of AMOC strength (McManus et al., 2004).

291 Heinrich Stadial 1 is associated with at least two major Iceberg Rafted Debris (IRD) discharges first
292 identified near the Iberian margin (Bard et al., 2000). They may reflect either the impact of changes in
293 ocean conditions on ice shelf and ice sheet stabilities (Alvarez-Solas et al., 2011). Alternatively, the
294 iceberg discharges themselves may have affected the AMOC, which is known to have major impacts
295 on patterns of sea surface temperature, sea ice, atmospheric circulation, and climate over surrounding
296 continents. The first IRD phase originated from ice sheet discharges from Northern Europe and Iceland,
297 causing strong reorganizations in deep circulation of the North East Atlantic (Stanford et al., 2011,
298 Grousset et al., 2001; Peck et al., 2006) while the second IRD phase is caused by discharges from the
299 Laurentide ice sheet. Recent studies (e.g. Hodell et al., 2017, Toucanne et al., 2015) suggest that all IRD
300 phases occur after 16.2 ka, during Heinrich Stadial 1 Phase 2. Before that, Heinrich Stadial Phase 1 is
301 associated with a strong increase of sediment fluxes due to meltwater arrival through terrestrial
302 terminating ice streams originating from both European and American sides of the North Atlantic as a
303 response to the beginning of the deglaciation (Toucanne et al., 2015, Ullman et al., 2015, Leng et al.,
304 2018) (Figure 3). During the first slowdown of AMOC during Phase 1 of Heinrich Stadial 1, the
305 associated warming of subsurface water would hence enable the destabilization of marine ice-shelves
306 occurring during Phase 2 (Alvarez-Solas et al., 2011; Marcott et al., 2011). This second phase of Heinrich
307 Stadial 1 is also associated with an extensive sea ice production, south of Greenland (Hillaire-Marcel
308 and de Vernal, 2008). The increase of North Atlantic sea ice extent and major iceberg discharges during
309 the second phase of Heinrich Stadial 1 are coherent with a southward shift of the evaporative region
310 providing moisture to Greenland supported by δ -excess data, and a southward shift of tropical
311 rainbelts (Chiang and Bitz, 2005), affecting southern hemisphere CH_4 sources (Rhodes et al., 2015).

312 **Conclusions**

313 Combined measurements of d-excess and ^{17}O -excess along the NGRIP ice core demonstrate a
314 decoupling between a cold and stable Greenland climate and changes in hydroclimate at lower
315 latitudes during the Heinrich Stadial 1, also referred to as the “Mystery Interval” (Denton et al., 2006).
316 These new measurements hence confirm the previous studies of Zhang et al. (2014, 2016) and Rhodes
317 et al. (2015). While Greenland temperature remains mostly stable from 20 to 14.7 ka, a large-scale
318 climatic reorganization takes place at 16.2 ka, associated with warmer and wetter conditions at the
319 location of Greenland moisture sources. Based on a coherent temporal framework linking the different
320 ice core records, we show that this event coincides with changes in the characteristics of the bipolar
321 seesaw pattern as observed in the Atlantic sector of Antarctica, and has a fingerprint in global
322 atmospheric composition through sharp changes in atmospheric CO_2 and CH_4 concentrations.

323 Based on these new ice core records and the comparison with marine and terrestrial records, we
324 propose the following sequence of events during the last deglaciation. First, the initiation of Heinrich
325 Stadial 1 occurs at 17.5 ka or earlier, with meltwater arrival from the terrestrial terminating ice-streams
326 synchronous with a decrease in the North Atlantic sea surface temperature off-shore Europe, a first
327 AMOC slowdown, drier conditions in North America, and an increase in Antarctic temperature as well
328 as in atmospheric CO_2 and CH_4 concentrations. No fingerprint of this first phase of Heinrich Stadial 1 is
329 identified in Greenland water stable isotope records: $\delta^{18}\text{O}$ (and thus local temperature), ^{17}O -excess
330 and d-excess remain stable. A possible explanation for such stability is that the high-latitude warming
331 induced by the increase in the summer insolation at high latitude over the beginning of the deglaciation
332 is counterbalanced in Greenland by regional changes in e.g. increased albedo due to sea ice extent or
333 reduced transport of heat by the atmospheric circulation towards central Greenland, which both can
334 result from a reduced AMOC strength. The global event occurring at 16.2 ka marks the onset of the
335 second phase of Heinrich Stadial 1. It is associated with (i) strong iceberg discharges due to dynamical
336 instability of the Laurentide ice sheet, probably induced by the accumulation of subsurface ocean heat
337 due to a slowdown of AMOC during Phase 1, (ii) a widespread reorganization of the atmospheric water
338 cycle in the Atlantic region, with significant changes in d-excess and ^{17}O -excess in Greenland, as well

339 as (iii) the initiation of weak monsoon interval in East Asia and (iv) the transition from a “big dry”
340 episode to a “big wet” episodes in North America. We note that this sequence of events within Heinrich
341 Stadial 1 is invisible in all available Greenland temperature proxy records, which only display an abrupt
342 warming at the onset of the Bølling-Allerød (14.7 ka).

343 Attached to a bipolar synchronized chronological framework, our new ice core data provide a unique
344 benchmark to test the ability of Earth System models (ESM) to correctly resolve the mechanisms
345 occurring at sub-millennial scale during the last deglaciation. In particular, our proposed sequence of
346 event is useful to evaluate ESM capabilities in reproducing the relationships between meltwater fluxes,
347 the state of the North Atlantic ocean circulation, the Laurentide ice sheet instability, changes at the
348 moisture sources of Greenland ice cores, the response of hydroclimate at low and high latitudes, as
349 well as the net quantitative effects on global methane and carbon budgets.

350 **Acknowledgements**

351 The research leading to these results has received funding from the European Research Council
352 under the European Union’s Seventh Framework Programme (FP7/2007-2013) / RC agreement
353 number 306045. E. C. is funded by the European Union's Seventh Framework Programme for
354 research and innovation under the Marie Skłodowska-Curie grant agreement no 600207. R.H.R.
355 received funding from a European Commission Horizon 2020 Marie Skłodowska-Curie Individual
356 Fellowship (no. 658120, SEADOG). We thank Myriam Guillevic and Jean Jouzel for very useful
357 discussions as well as Christo Buizert and an anonymous reviewer for very useful comments.

358

359 **References**

360 Álvarez-Solas, J., Montoya, M., Ritz, C., Ramstein, G., Charbit, S., Dumas, C., Nisancioglu, K., Dokken,
361 T. and Ganopolski, A.: Heinrich event 1: an example of dynamical ice-sheet reaction to oceanic
362 changes, *Clim. Past*, 7(4), 1297–1306, 2011

363 Andersen, K.K., Svensson, A., Johnsen, S.J., Rasmussen, S.O., Bigler, M., Roethlisberger, R., Ruth, U.,
364 Siggaard-Andersen, M.L., Steffensen, J.P., Dahl-Jensen, D., Vinther, B.M. and Clausen, H.B., The
365 Greenland Ice Core Chronology 2005, 15-42 ka. Part 1: constructing the time scale, *Quat. Sci. Rev.*,
366 25(23–24), 3246–3257, 2006

367 Asmerom, Y., Polyak, V.J. and Burns, S.J., Variable winter moisture in the southwestern United States
368 linked to rapid glacial climate shifts, *Nature Geosci.*, 3, 114-117, 2010

369 Bard, E., Rostek, F., Turon, J.L. and Gendreau, S.: Hydrological Impact of Heinrich Events in the
370 Subtropical Northeast Atlantic *Science*, 289, 1321–1324, 2000

371 Barkan, E. and Luz, B.: High precision measurements of 17O/16O and 18O/16O ratios in H2O, *Rapid*
372 *Commun., Mass Spectrom.*, 19(24), 3737–3742, 2005

373 Bauska, T.K., Baggenstos, D., Brook, E.J., Mix, A.C., Marcott, S. A. and Petrenko, V., Carbon isotopes
374 characterize rapid changes in atmospheric carbon dioxide during the last deglaciation, *PNAS*, 113(13),
375 3465-3470, 2016

376 Bazin, L., Landais, A., Lemieux-Dudon, B., Toyé Mahamadou Kele, H., Veres, D., Parrenin, P.
377 Martinerie, P., Ritz, C., Capron, E., Lipenkov, V., Loutre, M.F., Raynaud, D., Vinther, B., Svensson, A.,
378 Rasmussen, S.O., Severi, M., Blunier, T., Leuenberger, M., Fischer, H., Masson-Delmotte, V.,
379 Chappellaz, J. and Wolff, E.: An optimized multi-proxy, multi-site Antarctic ice and gas orbital
380 chronology (AICC2012): 120-800 ka, *Clim. Past*, 9(4), 1715–1731, 2013

381 Bonne, J.-L., H. C. Steen-Larsen, C. Risi, M. Werner, H. Sodemann, J.-L. Lacour, X. Fettweis, G. Cesana,
382 M. Delmotte, O. Cattani, P. Vallelonga, H. A. Kjaer, C. Clerbaux, A. E. Sveinbjornsdottir and V. Masson-
383 Delmotte: The summer 2012 Greenland heat wave: In situ and remote sensing observations of water
384 vapor isotopic composition during an atmospheric river event; *Journal of Geophysical Research-*
385 *Atmospheres*, 120(7), 2970-2989, 2015

386 Boyle, E. A.: Cool tropical temperatures shift the global $\delta^{18}\text{O-T}$ relationship: An explanation for the
387 ice core $\delta^{18}\text{O}$ -borehole thermometry conflict?, *Geophysical Research Letters*, 24(3), 273-276, 1994

388 Broecker, W. and Putnam, A.E.: How did the hydrologic cycle respond to the two-phase mystery
389 interval?, *Quat. Sci. Rev.*, 57(C), 17–2, 2012

390 Buiron, D., Stenni, B., Chappellaz, J., Landais, A., Baumgartner, M., Bonazza, M., Capron, E., Frezzotti,
391 M., Kageyama, M., Lemieux-Dudon, B., Masson-Delmotte, V., Parrenin, F., Schilt, A., Selmo, E., Severi,
392 M., Swingedouw, D. and Udisti, R.: Regional imprints of millennial variability during the MIS 3 period
393 around Antarctica, *Quat. Sci. Rev.*, 48, 99-112, 2012

394 Buizert, C., Gkinis, V., Severinghaus, J.P., He, F., Lecavalier, B. S., Kindler, P., Leuenberger, M., Carlson,
395 A.E., Vinther, B., Masson-Delmotte, V., White, J.W.C., Liu, Z., Otto-Bliesner and B., Brook, E.J.:
396 Greenland temperature response to climate forcing during the last deglaciation, *Science*, 345(6201),
397 1177–1180, 2014

398 Buizert, C., Keisling, B.A., Box, J.E., He, F., Carlson, A.E., Sinclair, G. and DeConto, R.M., Greenland-
399 Wide Seasonal Temperatures During the Last Deglaciation. *Geophys. Res. Lett.* 45, 1905-1914, 2018

400 Chiang, J. C. H. and Bitz, C.M.: Influence of high latitude ice cover on the marine Intertropical
401 Convergence Zone, *Clim. Dyn.*, 25(5), 477–496, 2005

402 Clark, P.U., Shakun, J.D., Baker, P.A., Bartlein, P.J., Brewer, S., Brook, E., Carlson, A.E., Cheng, H.,
403 Kaufman, D.S., Liu, Z., Marchitto, T.M., Mix, A.C., Morrill, C., Otto-bliesner, B.L., Pahnke, K., Russell,
404 J.M., Whitlock, C., Adkins, J.F., Blois, J.L., Clark, J., Colman, S. M., Curry, W. B., Flower, B. P., He, F.,
405 Johnson, T.C., Lynch-Stieglitz, J., Markgraf, V., Mcmanus, J., Mitrovica, J.X., Moreno, P.I. and Williams,
406 J.W.: Global climate evolution during the last deglaciation, *PNAS*, 109(19), E1134-E1142, 2012

407 Dahl-Jensen, D., Mosegaard, K., Gundestrup, N., Clow, G.D., Johnsen, S.J., Hansen, A.W. and Balling,
408 N.: Past Temperatures Directly from the Greenland Ice Sheet, *Science*, 282(5387), 268–271, 1998

409 Dansgaard, W.: Stable isotopes in precipitation, *Tellus*, 16, 436–468, 1964

410 Denton, G. H., Broecker, W.S. and Alley, R.B.: The mystery interval 17.5 to 14.5 kyrs ago PAGES news,
411 14(20), 14–16, 2006

412 Denton, G.H., Anderson, R.F., Toggweiler, J.R., Edwards, R.L., Schaefer, J.M. and Putnam, A.E.: The
413 Last Glacial Termination, *Science*, 328, 1652–1656, 2010

414 Deplazes, G., Luckge, A., Peterson, L.C., Timmermann, A., Hamann, Y., Hughen, K.A., Rohl, U., Laj, C.,
415 Cane, M.A., Sigman, D.M. and Haug, G.H., Links between tropical rainfall and North Atlantic climate
416 during the last glacial period, *Nature Geosci.*, 6, 213–217, 2013

417 Epica community members: One-to-one coupling of glacial climate variability in Greenland and
418 Antarctica, *Nature*, 444(7116), 195–198, 2006

419 Epstein, S., Buchsbaum, R., Lowenstam, H.A. and Urey, H.: Revised carbonate-water isotopic
420 temperature scale *GSA bulletin*, 64(11), 1315–1325, 1953

421 Gherardi, J.-M., Labeyrie, L., McManus, J.F., Francois, R., Skinner, L.C. and Cortijo, E.: Evidence from
422 the Northeastern Atlantic basin for variability in the rate of the meridional overturning circulation
423 through the last deglaciation, *Earth Planet. Sci. Lett.*, 240(3), 710–723, 2005

424 Grootes, P. M., Stuiver, M., White, J. W. C., Johnsen, S. and Jouzel, J.: Comparison of oxygen isotope
425 records from the GISP2 and GRIP Greenland ice cores, *Nature*, 366, 552–554, 1993

426 Grousset, F.: Les changements abrupts du climat depuis 60 000 ans / Abrupt climatic changes over
427 the last 60,000 years, *Quaternaire*, 12(4), 203–211, 2001

428 Guillevic, M., Bazin, L., Landais, A., Stowasser, C., Masson-Delmotte, V., Blunier, T., Eynaud, F.,
429 Falourd, S., Michel, E., Minster, B., Popp, T., Prié, F. and Vinther, B. M.: Evidence for a three-phase
430 sequence during Heinrich Stadial 4 using a multiproxy approach based on Greenland ice core records,
431 *Clim. Past*, 10, 2115–2133, 2014

432 Hillaire-Marcel, C. and De Vernal, A.: Stable isotope clue to episodic sea ice formation in the glacial
433 North Atlantic, *Earth Plan. Sci. Lett.*, 268, 143–150, 2008

434 Hoff U, Rasmussen TL, Stein R, Ezat MM, Fahl K. Sea ice and millennial-scale climate variability in the
435 Nordic seas 90 kyr ago to present. *Nat Commun.*, 7, 12247, 2016.

436 Hodell, D.A., Nicholl, J.A., Bontognali, T.R.R., Danino, S., Dorador, J., Dowdeswell, J.A., Einsle, J.,
437 Kuhlmann, H., Martrat, B., Mleneck-vautravers, M.J., Rodríguez-tovar, F.J. and Röhl, U.: Anatomy of
438 Heinrich Layer 1 and its role in the last deglaciation, *Paleoceanography and Paleoclimatology*, 32(3),
439 10.1002/2016PA003028, 2017

440 Johnsen, S. J., Dansgaard, W. and White, J.W.C.: The origin of Arctic precipitation under present and
441 glacial conditions, *Tellus B*, 41B(4), 452–468, 1989

442 Jones, T. R., Roberts, W. H. G., Steig, E.J., Cuffey, K.M., Markle, B.R. and White, J.W.C.: Southern
443 Hemisphere climate variability forced by Northern Hemisphere ice-sheet topography, *Nature*, 554,
444 351–355, 2018

445 Jouzel, J., Merlivat, L. and Lorius, C.: Deuterium excess in an East Antarctic ice core suggests higher
446 relative humidity at the oceanic surface during the last glacial maximum, *Nature*, 299, 688-691, 1982

447 Jouzel, J., Masson-Delmotte, V., Stiévenard, M. and Landais, A.: Rapid deuterium-excess changes in
448 Greenland ice cores : a link between the ocean and the atmosphere, *Comptes Rendus - Geosci.*, 337,
449 957–969, 2005

450 Kindler, P., Guillevic, M., Baumgartner, M., Schwander, J., Landais, A. and Leuenberger, M.:
451 Temperature reconstruction from 10 to 120 kyr b2k from the NGRIP ice core, *Clim. Past*, 10(2), 887–
452 902, 2014

453 Klein, E.S., Cherry, J.E., Young, J., Noone, D., Leffler, A.J. and Welker, J.M.: Arctic cyclone water vapor
454 isotopes support past sea ice retreat recorded in Greenland ice Sci. Rep.5: 10295-10300, 2015

455 Kopec, B.G., Feng, X., Michel, F.A. and Posmentier, E.S., Influence of sea ice on Arctic precipitation
456 *Proc. Natl. Acad. Sci.*, 113(1), 46–51, 2016

457 Krinner, G., Genthon, C. and Jouzel, J.: GCM analysis of local influences on ice core δ signals.
458 *Geophysical Research Letters*, 24(22), 2825-2828, 1997

459 Landais, A., Barkan, E. and Luz, B.: Record of $\delta^{18}\text{O}$ and ^{17}O -excess in ice from Vostok Antarctica during
460 the last 150,000 years, *Geophys. Res. Lett.* 35(2): L02709, 2008

461 Landais, A., Steen-Larsen, H.C., Guillevic, M., Masson-Delmotte, V., Vinther and B., Winkler, R.: Triple
462 isotopic composition of oxygen in surface snow and water vapor at NEEM (Greenland) *Geochim.*
463 *Cosmochim. Acta*, 77, 304–316, 2012

464 Landais, A., Winkler, R. and Prié, F., Triple Isotopic Composition of Oxygen in Water from Ice Cores,
465 application note 30287, Thermo, 2014

466 Langen, P.L. and Vinther, B.M.: Response in atmospheric circulation and sources of Greenland
467 precipitation to glacial boundary conditions, *Clim. Dyn.*, 32(7–8), 1035–1054, 2009

468 Leng W, von Dobeneck T, Bergmann F, Just J., Mulitza S., Chiessi C., St-Onge G. and Piper D.:
469 Sedimentary and rock magnetic signatures and event scenarios of deglacial outburst floods from the
470 Laurentian Channel Ice Stream, *Quat Sci Rev.*, 186, 27-46,
471 doi:<https://doi.org/10.1016/j.quascirev.2018.01.016>, 2018

472 Marcott, S.A., Clark, P.U., Padman, L., Klinkhammer, G.P., Springer, S.R., Liu, Z., Otto-Bliesner, B.L.,
473 Carlson, A.E., Ungerer, A., Padman, J., He, F., Cheng, J. and Schmittner, A., Ice-shelf collapse from
474 subsurface warming as a trigger for Heinrich events, *Proc. Natl. Acad. Sci. U. S. A.*, 2011

475 Marcott, S. A, Bauska, T.K., Buizert, C., Steig, E.J., Rosen, J.L., Cuffey, K.M., Fudge, T.J., Severinghaus,
476 J.P., Ahn, J., Kalk, M.L., McConnell, J.R., Sowers, T., Taylor, K. C., White, J.W.C. and Brook, E.J.:
477 Centennial-scale changes in the global carbon cycle during the last deglaciation, *Nature*, 514(7524),
478 616–619, 2013

479 Markle, B.R., Steig, E. J., Buizert, C., Schoenemann, S. W., Bitz, C. M., Fudge, T. J., Pedro, J. B., Ding,
480 Q., Jones, T.R., White, J.W.C. and Sowers, T.: Global atmospheric teleconnections during Dansgaard–
481 Oeschger events, *Nat. Geosci.* 10(1), 36–40, 2016

482 Martrat, B., Jimenez-Amat, P., Zahn, R. and Grimalt, J.O.: Similarities and dissimilarities between the
483 last two deglaciations and interglaciations in the North Atlantic region, *Quat. Sci. Rev.*, 99, 122–134,
484 2014

485 Masson-Delmotte, V., Landais, A., Stievenard, M., Cattani, O., Falourd, S., Jouzel, J., Johnsen, S. J.
486 Dahl-Jensen, D., Sveinbjornsdottir, A., White, J.W.C., Popp, T. and Fischer, H., Holocene climatic
487 changes in Greenland: Different deuterium excess signals at Greenland Ice Core Project (GRIP) and
488 NorthGRIP, *J. Geophys. Res. D Atmos.*, 110(14), 1–13, 2005a

489 Masson-Delmotte, V., Jouzel, J., Landais, A., Stievenard, M., Johnsen, S.J., White, J.W.C., Werner, M.,
490 Sveinbjornsdottir, A. and Fuhrer, K.: GRIP deuterium excess reveals rapid and orbital-scale changes in
491 Greenland moisture origin, *Science*, 309(5731), 118–121, 2005b

492 McManus, J. F., Francois, R., Gherardi, J.-M., Keigwin, L.D. and Brown-Leger S.: Collapse and rapid
493 resumption of Atlantic meridional circulation linked to deglacial climate changes, *Nature*, 428(6985),
494 834–837, 2004

495 NGRIP community members, High-resolution climate record of Northern Hemisphere climate
496 extending into the last interglacial period, *Nature*, 431, 147–151, 2004

497 Partin, J. W., Cobb, K. M., Adkins, J. F., Clark, B. and Fernandez, D. P.: Millennial scale trends in west
498 Pacific warm pool hydrology since the Last Glacial Maximum, *Nature*, 449, 452–455, 2007.

499 Peck, V. L., Hall, I.R., Zahn, R., Elderfield, H. and Grousset, F.: High resolution evidence for linkages
500 between NW European ice sheet instability and Atlantic Meridional Overturning Circulation, *Earth
501 Plan. Sci. Let.*, 243, 476–488, 2006

502 Pfahl, S. and Sodemann, H.: What controls deuterium excess in global precipitation?, *Clim. Past* 10(2),
503 771–781, 2014

504 Rasmussen, S.O., Andersen, K.K., Svensson, A.M., Steffensen, J.P., Vinther, B.M., Clausen, H.B.,
505 Siggaard-Andersen, M.L., Johnsen, S.J., Larsen, L.B., Dahl-Jensen, D., Bigler, M., Roethlisberger, R.,
506 Fischer, H., Goto-Azuma, K., Hansson, M.E. and Ruth, U.: A new Greenland ice core chronology for
507 the last glacial termination, *J. Geophys. Res. Atmos.*, 111(6), 1–16, 2006

508 Rasmussen, S.O., Seierstad, I.K., Andersen, K.K., Bigler, M. and Johnsen, S.J.: Synchronization of the
509 NGRIP , GRIP , and GISP2 ice cores across MIS 2 and palaeoclimatic implications, *Quat. Sci. Res.*, 27,
510 18–28, 2008

511 Rhines, A. and Huybers, P.J.: Sea ice and dynamical controls on preindustrial and last glacial
512 maximum accumulation in central Greenland *J. Clim.* 27(23): 8902–8917, 2014

513 Rhodes, R.H., Brook, E.J., Chiang, J. C. H., Blunier, T., Maselli, O.J., McConnell, J., Romanini, D. and
514 Severinghaus, J.P.: Enhanced tropical methane production in response to iceberg discharge in the
515 North Atlantic, *Science*, 348(6238), 1016–1019, 2015

516 Risi, C., Landais, A., Bony, S., Jouzel, J., Masson-Delmotte, V. and Vimeux, F.: Understanding the ¹⁷O
517 excess glacial-interglacial variations in Vostok precipitation, *J. Geophys. Res. Atmos.*, 115(10),
518 D10112, 2010

519 Russell, J., Vogel, H., Konecky, B.L., Bijaksana, S., Huang, Y., Melles, M., Wattrus, N., Costa, K. and
520 King, J.W.: Glacial forcing of central Indonesian hydroclimate since 60,000 y BP., *Proc. Natl Acad. Sci.*,
521 111, 5100–5105, 2014

522 Schoenemann, S. W., Schauer, S. and Steig, E.J.: Measurement of SLAP2 and GISP d17O and proposed
523 VSMOW-SLAP normalization for d17O and ¹⁷Oexcess, *Rapid Commun. Mass Spectrom.*, 27(5), 582–
524 590, 2013

525 Schoenemann, S.W., Steig, E.J., Ding, Q., Markle, B.R. and Schauer, A.J.: Triple water-isotopologue
526 record from WAIS Divide, Antarctica: Controls on glacial-interglacial changes in ¹⁷O-excess of
527 precipitation, *J. Geophys. Res. Atmos.*, 119(14), 8741–8763, 2014

528 Schoenemann, S.W. and Steig, E.J.: Seasonal and spatial variations of ¹⁷O-excess and d-excess in
529 Antarctic precipitation: Insights from an intermediate complexity isotope model, *J. Geophys. Res.*
530 *Atmos.*, 121(19), 11,211-215,247, 2016

531 Severinghaus, J. P. and Brook, E.: Abrupt climate change at the end of the last glacial period inferred
532 from trapped air in polar ice, *Science*, 286 (5441), 930-934, 1999

533 Stanford, D., Rohling, E. J., Bacon, S., Roberts, A.P., Grousset, F.E. and Bolshaw, M.: A new concept for
534 the paleoceanographic evolution of Heinrich event 1 in the North Atlantic, *Quat. Sci. Rev.*, 30(9–10),
535 1047–1066, 2011

536 Steffensen, J. P., Andersen, K.K., Bigler, M., Clausen, H.B., Dahl-Jensen, D., Fischer, H., Goto-Azuma,
537 K., Hansson, M., Johnsen, S.J., Jouzel, J., Masson-Delmotte, V., Popp, T., Rasmussen, S.O.,
538 Rothlisberger, R., Ruth, U., Stauffer, B., Siggaard-Andersen, M.-L., Sveinbjörnsdóttir, A. E., Svensson,
539 A. and White, J.W.C., High-Resolution Greenland Ice Core Data Show Abrupt Climate Change
540 Happens in Few Years *Science*, 321(5889), 680-684, 2008

541 Stenni, B., Buiron, D., Frezzotti, M., Albani, S., Barbante, C., Bard, E., Barnola, J.M., Baroni, M.,
542 Baumgartner, M., Bonazza, M., Capron, E., Castellano, E., Chappellaz, J., Delmonte, B., Falourd, S.,
543 Genoni, L., Iacumin, P., Jouzel, J., Kipfstuhl, S., Landais, A., Lemieux-Dudon, B., Maggi, V., Masson-
544 Delmotte, V., Mazzola, C., Minster, B., Montagnat, M., Mulvaney, R., Narcisi, B., Oerter, H., Parrenin,
545 F., Petit, J.R., Ritz, C., Scarchilli, C., Schilt, A., Schüpbach, S., Schwander, J., Selmo, E., Severi, M.,
546 Stocker, T.F. and Udisti, R.: Expression of the bipolar see-saw in Antarctic climate records during the
547 last deglaciation, *Nat. Geosci.*, 4(1), 46-49, 2011

548 Stríkis, N.M., Chiessi, C.M., Cruz, F.W., Vuille, M., Cheng, H., De Souza Barreto, E.A., Mollenhauer, G.,
549 Kasten, S., Karmann, I., Edwards, R.L., Bernal, J.P. and Sales, H.D.R.: Timing and structure of Mega-
550 SACZ events during Heinrich Stadial 1, *Geophys. Res. Lett.*, 42 (13), 5477–5484, 2015.

551 Svensson, A., Andersen, K.K., Bigler, M., Clausen, H.B., Dahl-Jensen, D., Davies, S.M., Johnsen, S.J.,
552 Muscheler, R., Parrenin, F., Rasmussen, S.O., Röthlisberger, R., Seierstad, I., Steffensen, J.P. and
553 Vinther, B.M.: A 60 000 year Greenland stratigraphic ice core chronology, *Clim. Past*, 4 (1), 47–57,
554 2008

555 Toucanne, S., Zaragosi, S., Bourillet, J.-F., Marieu, V., Cremer, M., Kageyama, M., Van Vliet-Lanoë, B.,
556 Eynaud, F., Turon, J.-L. and Gibbard, P.-L.: The first estimation of Fleuve Manche palaeoriver
557 discharge during the last deglaciation: Evidence for Fennoscandian ice sheet meltwater flow in the
558 English Channel ca 20-18 ka ago, *Earth Planet. Sci. Lett.*, 290(3–4), 459–473, 2010

559 Toucanne, S., Soulet, G., Freslon, N., Silva Jacinto, R., Dennielou, B., Zaragosi, S., Eynaud, F., Bourillet,
560 J.-F. and Bayon, G.: Millennial-scale fluctuations of the European Ice Sheet at the end of the last
561 glacial, and their potential impact on global climate, *Quaternary Science Reviews*, 123, 113-133, 2015

562 Touzeau, A., Landais, A., Stenni, B., Uemura, R., Fukui, K., Fujita, S., Guilbaud, S., Ekaykin, A., Casado,
563 M., Barkan, E., Luz, B., Magand, O., Teste, G., Le Meur, E., Baroni, M., Savarino, J., Bourgeois, I. and
564 Risi, C.: Acquisition of isotopic composition for surface snow in East Antarctica and the links to
565 climatic parameters, *The Cryosphere*, 10, 837–852, 2016

566 Uemura, R., Masson-Delmotte, V., Jouzel, J., Landais, A., Motoyama, H. and Stenni, B.: Ranges of
567 moisture-source temperature estimated from Antarctic ice cores stable isotope records over glacial–
568 interglacial cycles, *Clim. Past* 8(3), 1109–1125, 2012

569 Ullman, D.J., Carlson, A.E., Anslow, F.S., LeGrande, A.N. and Licciardi, J.M.: Laurentide ice-sheet
570 instability during the last deglaciation, *Nat. Geosci.*, 8(7), 534-537, 2015

571 Vaughn, B., H., White, J.W.C., Delmotte, M., Trolier, M., Cattani, O. and Stievenard, M.: An
572 automated system for hydrogen isotope analysis of water, *Chemical Geology Including Isotope*
573 *Geoscience*, 152, 309-319, 1998

574 Veres, D., Bazin, L., Landais, A., Toyé Mahamadou Kele, H., Lemieux-Dudon, B., Parrenin, P.,
575 Martinerie, P., Blayo, E., Blunier, T., Capron, E., Chappellaz, J., Rasmussen, S.O., Severi, M., Svensson,
576 A., Vinther, B. and Wolff, E.W., The Antarctic ice core chronology (AICC2012): an optimized multi-
577 parameter and multi-site dating approach for the last 120 thousand years, *Clim. Past*, 9(4), 1733–
578 1748, 2013

579 Wais Divide Members: Onset of deglacial warming in West Antarctica driven by local orbital forcing
580 *Nature*, 500(7463), 440–444, 2013

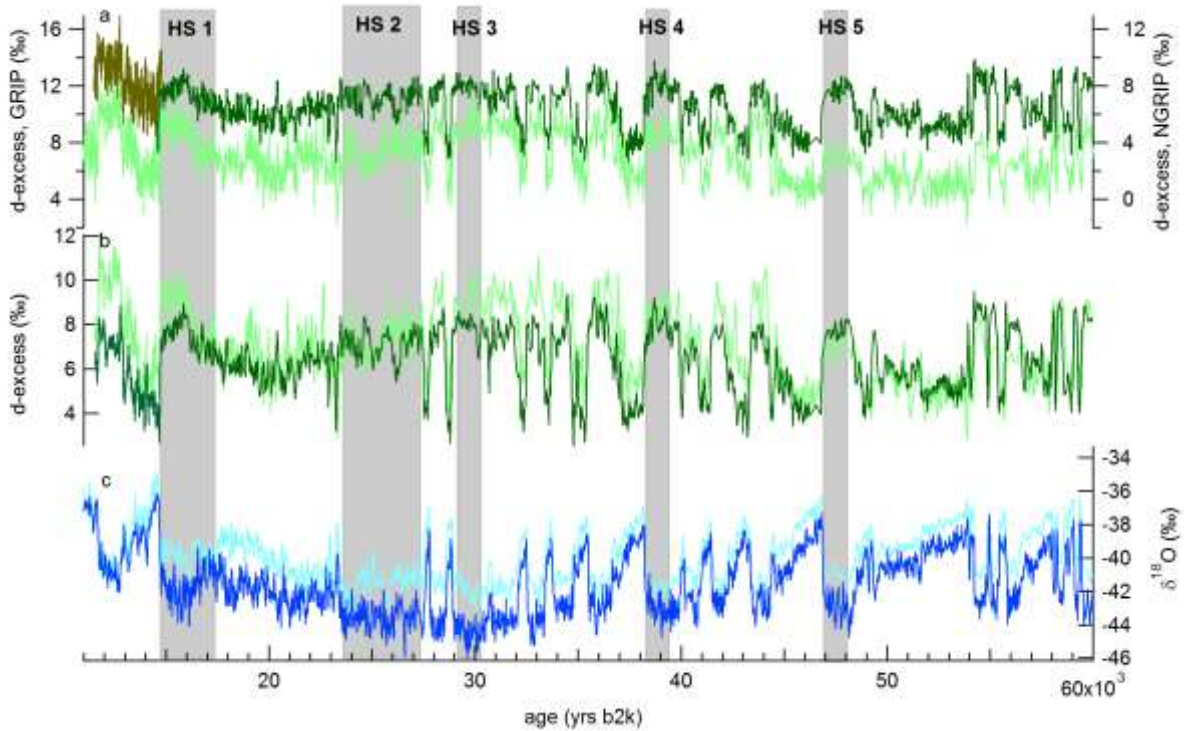
581 Werner, M., Heimann, M. and Hoffmann, G. Isotopic composition and origin of polar precipitation in
582 present and glacial climate simulations, *Tellus B: Chemical and Physical Meteorology*, 53(1), 53-71,
583 2001

584 Winkler, R., Landais, A., Sodemann, H., Dümbgen, L., Prié, F., Masson-Delmotte, V., Stenni, B. and
585 Jouzel, J.: Deglaciation records of ¹⁷O-excess in East Antarctica: Reliable reconstruction of oceanic
586 normalized relative humidity from coastal sites, *Clim. Past*, 8(1), 1–16, 2012

587 Zhang, W., Wu, J., Wang, Y., Wang, Y., Cheng, H., Kong, X. and Duan, F. A: detailed East Asian
588 monsoon history surrounding the ‘Mystery Interval’ derived from three Chinese speleothem records,
589 *Quat. Res.*, 82(1), 154–163, 2014

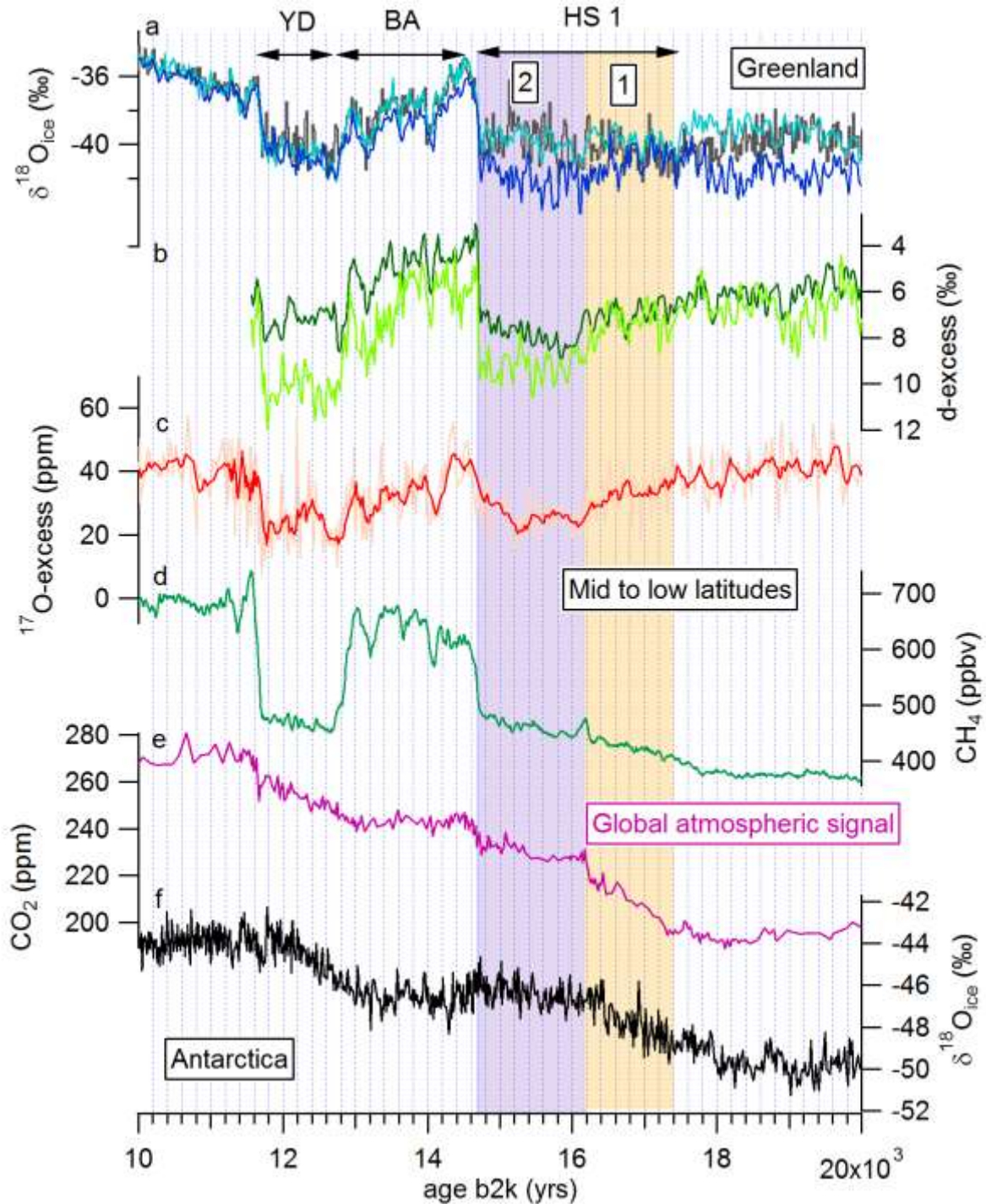
590 Zhang, H., Griffiths, M.L., Huang, J., Cai, Y., Wang, C., Zhang, F., Cheng, H., Ning, Y., Hu, C. and Xie, S.,
591 Antarctic link with East Asian summer monsoon variability during the Heinrich Stadial–Bølling
592 interstadial transition. *Earth Planet. Sci. Lett.* 453, 243-251, 2016

593



594

595 **Figure 1:** water stable isotope records ($\delta^{18}O$ and d -excess, in ‰) from GRIP and NGRIP ice cores
 596 reported on the GICC05 chronology (in thousands of years before year 2000 CE). a- d -excess from the
 597 NGRIP ice core (khaki: data obtained at INSTAAR SIL, Steffensen et al., 2008; dark green: data obtained
 598 at LSCE, this study); d -excess from the GRIP ice core (light green, Masson-Delmotte et al., 2005); b- d -
 599 excess from the NGRIP ice core after correction of the shift between INSTAAR SIL and LSCE (dark green)
 600 dataset, and d -excess from the GRIP ice core (light green); c- $\delta^{18}O$ from the NGRIP ice core (dark blue)
 601 datasets, $\delta^{18}O$ from the GRIP ice core (light blue).
 602 Grey intervals display Heinrich Stadials (HS).
 603

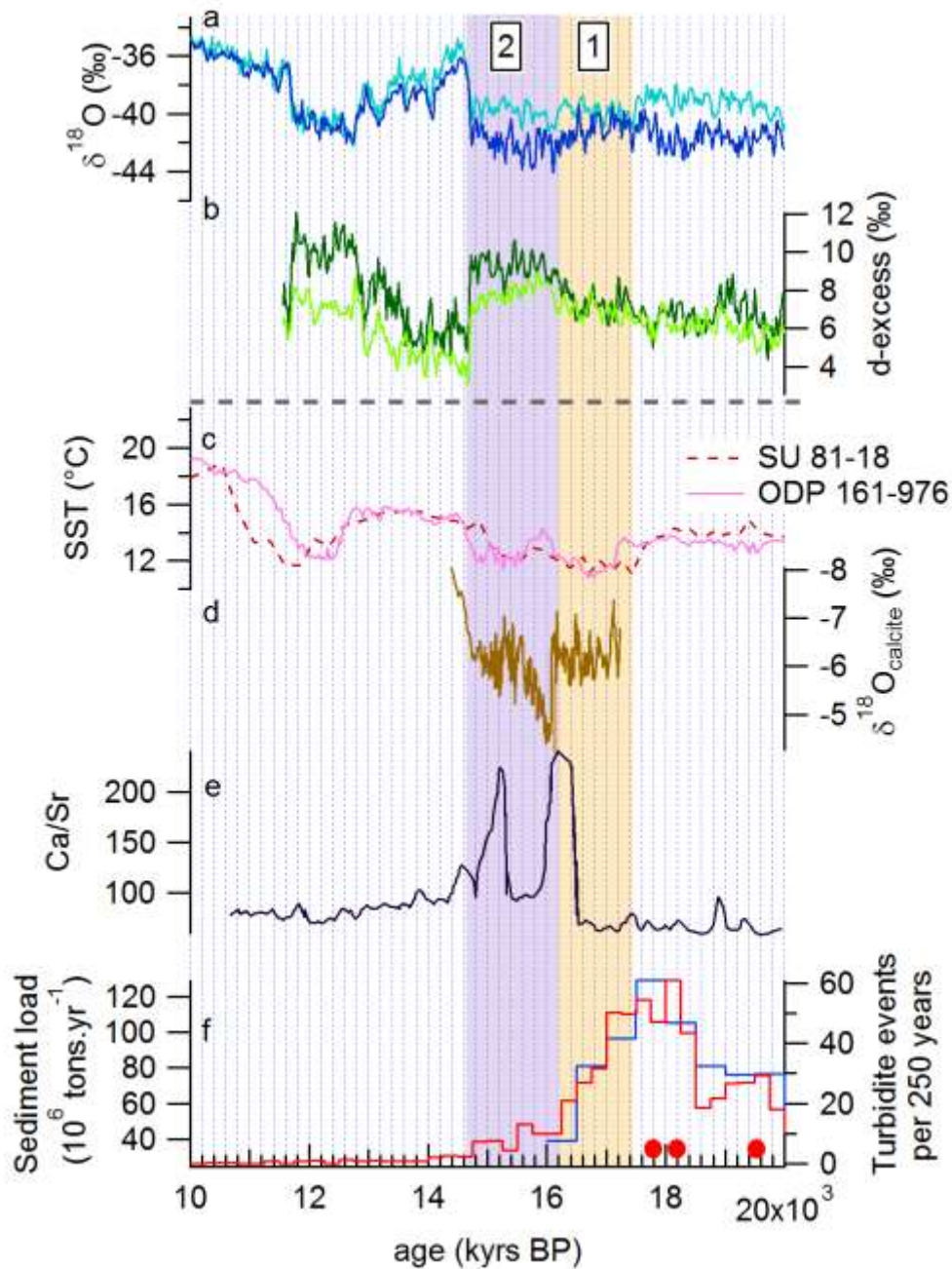


605

606 *Figure 2: A synthesis of ice core records over the last deglaciation displayed on the respective GICC05*
 607 *and AICC2012 timescales with an identification of two phases (1, orange box and 2, purple box) within*
 608 *Heinrich Stadial 1 (HS1) as discussed in the text: we locate the transition between phases 1 and 2 at the*
 609 *timing of the sharp increase in CO₂ and CH₄ concentrations, both being global atmospheric composition*
 610 *signals. The Younger Dryas (YD) and Bølling-Allerød (BA) periods are also indicated.*

611 *a-GRIP, NGRIP and GISP2 $\delta^{18}\text{O}$ (light blue, dark blue and black respectively (Grootes et al., 1993; NGRIP*
 612 *community members, 2004) interpolated at a 20 years resolution; b-GRIP and NGRIP d-excess (light and*

613 *dark green respectively: Jouzel et al., 2005, this study) interpolated at a 20 years resolution;c-NGRIP*
614 *¹⁷O-excess (orange curve shows the original series and the red curve the 5 years running average, this*
615 *study);d-WAIS Divide CH₄ (Rhodes et al., 2015);e-WAIS Divide CO₂ (Marcott et al., 2013);f-EPICA*
616 *Dronning Maud Land (EDML) δ¹⁸O_{ice} (EPICA community members, 2006)*
617



618
 619 **Figure 3:** The sequence of Phase 1 and Phase 2 of Heinrich Stadial 1 identified in Greenland records
 620 and in proxy records of North Atlantic SST, IRD events, and changes in East Asian hydroclimate. a-
 621 NGRIP (dark blue) and GRIP (light blue) $\delta^{18}\text{O}$ records; b- NGRIP (dark green) and GRIP (light green) d-
 622 excess records; c- Sea surface temperature (SST) for North Atlantic cores SU 81-18 (Bard et al., 2000)
 623 and ODP 161-976 (Martrat et al., 2014); d- Calcite $\delta^{18}\text{O}$ of Hulu cave (China, Zhang et al., 2014); e-
 624 Ca/Sr from site U1308 in the IRD belt (Hodell et al., 2019) as signature from strong iceberg discharges
 625 from the Laurentide ice sheet; f- Indications for Channel River sediment load (blue, sediment load;
 626 red, turbidite frequency) (Toucanne et al., 2010; 2015) as signature for meltwater input from
 627 European side.

628 The three red circles indicate plumite layers resulting from outburst floods on the Eastern Canadian
 629 margin (Leng et al., 2018), i.e. meltwater arrival from the North America side in the absence of strong
 630 iceberg discharge.

631 *The dashed horizontal line separates the ice core records reported on the GICC05 timescale from non*
632 *ice core records displayed on their own timescales.*

633

634

635